ISSN 2278-3091
Volume 8, No.1.6, 2019
International Journal of Advanced Trends in Computer Science and Engineering
Available Online at http://www.warse.org/IJATCSE/static/pdf/file/ijatcse5981.62019.pdf
https://doi.org/10.30534/ijatcse/2019/5981.62019

Single-phase Shunt Active Power Filter by Using Piecewise Linear Look-up Table Controller

Yushaizad Yusof[1], Aini Hussain[1], Mohd. Faisal Ibrahim[1], Anuar Mikdad Muad[1], Muhammad Ammirrul Attiqi Mohd Zainuri[1]
[1]INTEGRA, Fakulti Kejuruteraan & Alam Bina, Universiti Kebangsaan Malaysia, 43600 UKM Bangi, Selangor, Malaysia, yushaizad@eng.ukm.my, draini@ukm.edu.my, faisal.ibrahim@ukm.edu.my, anuar_muad@ukm.edu.my, ammirrulattiqi@ukm.edu.my

ABSTRACT

This paper elaborates the design and usefulness of piecewise linear look-up table based single input Fuzzy Logic controller as the compensator of single-phase shunt active power filter to overcome the source current harmonic problems. The MATLAB Simulink simulation results validate the effectiveness in mitigating the current total harmonics distortion under 5% and improved the system power factor to a near unity.

Key words: Active power filter, current harmonic, Fuzzy-PI controller, look-up table.

1. INTRODUCTION

The presence of current harmonic in the distribution power system in particular has contributed to additional power disturbances in the system. Typical current harmonic waveform feature is distorted and deviated from sinusoidal waveform. It is caused by the nonlinear loads which mainly comprises of power electronics devices, e.g. rectifier circuit with inductive load. Although its magnitude is not so great as compared to the other type of power disturbances but its occurrence is the most frequent and comprehensive. As a result, the effects that related to the current harmonic are reduction of system efficiency, power losses, reduction of system power factor, the heating of conductor, malfunction of sensitive equipment and so on. These effects must be addressed comprehensively in order to improve the system efficiency and reliability. One way to overcome the problems created by current harmonic is by the introduction of active power filter (APF) system [1]-[3].

The implementation of APF is the viable solution in tackling the current harmonic distortion issues in distribution power system [4]. Since substantial source of current harmonic comprises of single-phase nonlinear loads, many researchers adopted a single-phase APF configuration to mitigate current harmonic. There are two distinct APF configurations choice, i.e. shunt or series connection with the line, another one is the combination of both connections, which famously known as unified power quality conditioner (UPQC). There are many factors are taken into consideration prior to the APF configuration selection, such as harmonic detection method, current or voltage-controlled technique, development cost, number of solutions other than harmonic mitigation etc. The adopted single-phase APF circuit is basically a H-bridge inverter circuit with a DC-link capacitor and a filter inductor as energy storage elements. Usually a shunt APF (SAPF) is selected, since the connection between the SAPF and the line is direct at point of common coupling without a requirement of injection device [5].

Basically, the harmonic detection method based on time domain is preferred by many researchers compares to its counterpart, the frequency domain, mainly owing to its speed and simplicity in algorithm structure. The time domain harmonic detection method can be classified into current and voltage-controlled technique. This simply can be identified from the APF connection to the line, i.e. current control for shunt connection, whilst series connection for voltage control. Moreover, in case of current control, there are divided into two different methods, i.e. direct current control (DCC) and indirect current control (ICC) method. The DCC method is widely chosen for SAPF application because of many reasons, however the ICC method has an advantage of simpler control structure and requires only three sensors at least [6]. By selecting the DC load voltage and current as inputs, the nonlinear load equivalent resistance control strategy is applied as the control strategy to mitigate current harmonic and compensate reactive power [7].

The DCC method involves three steps. The first step is the harmonic detection method, followed by the compensator design to control the compensated current, and finally the pulse width modulation (PWM) switching scheme. The compensator design is very important in the APF control strategy since it determines the compensated current signal, regulates the system dynamic response and stability. Amongst specified dynamic response parameters to be investigated are

rise time, peak time, settling time, overshoot, damping ratio, steady state error etc. To attain satisfactory dynamic response, the compensator gains and variables must be precisely tuned and accurately analyzed.

Normally, a proportional plus integral (PI) controller is implemented as the compensator for APF [6]-[7]. The PI controller is a simple first order system which offers quite fast response with zero steady state error. Moreover, it is very popular and has been widely used in industrial control process as well as many other control automation and application. On the other hand, with the emerging of artificial intelligence (AI) based technology, e.g. Fuzzy Logic Controller (FLC), Expert System, Artificial Neural Network (ANN) have introduced an alternative to PI compensator, and have been implemented in many power electronics applications recently. This includes incorporates the FLC as the compensator in the APF [1]-[2], [8]-[9]. Besides, the ANN is used to generate a sinusoidal reference current for APF [10].

Since PI compensator requires a complete and precise mathematical model of the APF system in tuning its gains of proportional k_p and integral k_i, some researchers opt to FLC, due to its nonlinear nature, less requirement on precise mathematical model for designing and tuning, and furthermore it works well using imprecise inputs, as well as effectively handles nonlinear system [8]-[9]. Conversely the FLC has its own shortcomings such as the lack of a standard design procedure and usually is designed using heuristic manner, a time consuming for design, and inconsistency in obtaining a good performance [11]. A mixture of a PI controller and a FLC design yields a hybrid controller, known as the Fuzzy PI Controller (FPIC). This particular controller demonstrates a same small-signal performance to PI controller but has superior dynamic response for large-signal disturbances [12]. Moreover, in order to decrease more on the rule table membership functions and complexity of FPIC, a single input Fuzzy PI controller (SIFPIC) is introduced [13]. The SIPFIC is achieved by employing a 'signed distance method', which will have only a single input instead of two inputs for typical FLC, hence can simplify the FPIC control surface to a piecewise linear approximation [11], [14]. This technique has been implemented in APF, that proved its capability in compensating reactive power and successfully mitigating current harmonic distortion [2]. The first objective of this paper is to apply the harmonic detection method proposed in [7] and using PL-LTC as the compensator of SAPF. In addition, its performance is evaluated based on the achievement of a total harmonic distortion (THD) index of source current and the improvement of system power factor. Moreover, to validate the effectiveness of the compensator, a comparison between the proposed controller with the PI controller is carried out.

Based on these arguments, this paper presents the single-phase SAPF using piecewise linear look-up table controller. It applies the DCC method and using piecewise linear approximation based on a look-up table controller (PL-LTC) for the SAPF. Therefore, this paper is organized as follows; after the introduction section, the proposed methodology of control design is explained and implemented, next the performance of SAPF is verified using a MATLAB Simulink simulation tool. Finally, several simulation results are discussed and analyzed to verified the effectiveness of the proposed controller before the paper is closed with conclusion section. This study discusses and introduces the new controller for the SAPF which is based on a simplified PI-Fuzzy controller, its performance is comparable, and to some extent is better than the PI controller.

2. METHODOLOGY

The design of PL-LTC technique and its implementation as part of DCC method for SAPF is discussed and explained thoroughly in this section. Thus, this section shows some specific figures, tables and accompanied by the derivation of mathematical expression that represents the SAPF system and PL-LTC design.

2.1 Symmetrical PL-LTC Design

Fuzzy Logic is defined as a theory of vagueness and uncertainties. It provides an approximate but effective in describing the system behavior. Generally, the FPIC is applied in many control applications compared to the other type of FLCs [11]-[15]. This is because it inherits the PI controller characteristics as well as the advantage of FLC, which is simpler, more applicable as well as guarantees zero steady state error.

It is common for the FLC rule table having the error, e and change of error, $\dot{e}$ as the inputs to have the same output membership functions and is arranged in a diagonal direction. Usually, both crisp inputs will be normalized prior to be fuzzified. After the process of fuzzification, the inputs will be evaluated and decided using a predetermined rule table. Then it will undergo a defuzzification process, in order to return to a crisp value. This output signal which is in a form of differential value need to be denormalized first, before being integrated to yield a finished control signal. Often the rule table exhibits Toeplitz matrix or diagonal-constant matrix characteristics, where each point on a particular diagonal line has a magnitude that is proportional to the distance between the main diagonal line [11]. Therefore, in order to simplify the FPIC, instead of using two variable input sets (e and $\dot{e}$), a single input is used, which can be realized using the signed distance method [13]. This method reduces the number of inputs to a sole input variable known as a signed distance, d. The distance represents the absolute distance magnitude of each parallel diagonal lines (where e and $\dot{e}$ lies) from the main diagonal line, and is defined as:

$$d = \frac{\lambda e + \dot{e}}{\sqrt{1+\lambda^2}} \quad (1)$$

where, λ is defined as the slope of the main diagonal line.

Thus, for FPIC that has 49 rules can be shrink to only 7 rules. As a result, a single dimension (1-D) rule table can be formed, such as depicted in Table 1 [11]. As a result, the computation time can be made faster. The control surface output is the change in control output, $\dot{y}$. With this regard, the control surface output relates to the signed distance is:

$$\dot{y} = f(d) \quad (2)$$

Hence, $\dot{y}$ is the function of d, which indicates a linear function with a constant slope. The shape of control surface is determined by the peak locations of the input and the output membership functions.

In single input single output SIFPIC, the relationship of input and output can be mapped into a piecewise linear approximation using PL-LTC, as depicted in Figure 1 [11]-[14]. Apparently, the slope λ is 1, since every increment point for$d$ will result in identical point for $\dot{y}$. The range limit for the look-up table is [-100,100] for both $\dot{y}$ and d. It depends on the normalized value determined previously [15]. Thus, Table 2 shows the input-output membership values, which having the crisp values instead of the linguistic values. The difference between Table 1 and Table 2 is the output values, which indicates Table 1 is based on Mamdani type inference while Table 2 is based on Takagi-Sugeno type inference.

Table 1: Reduced rule table for FPIC

d	L_{NB}	L_{NM}	L_{NS}	L_Z	L_{PS}	L_{PM}	L_{PB}
$\dot{y}$	NB	NM	NS	Z	PS	PM	PB

Table 2: Reduced rule table for PL-LTC

d	L_{NB}	L_{NM}	L_{NS}	L_Z	L_{PS}	L_{PM}	L_{PB}
$\dot{y}$	-100	-66.7	-33.3	0	33.3	66.7	100

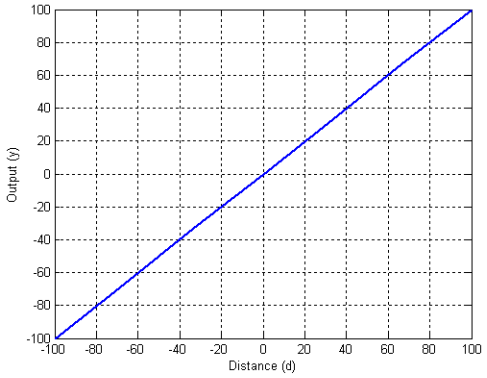

Figure 1: Symmetrical PL-LTC control surface

2.2 Compensator Design Using PL-LTC

As depicted in Figure 2, the compensator is drived by the error e which is the difference between reference compensated current and actual compensated current. Using the technique introduced in [7], the reference compensated current is generated. The system to be compensated is a first order system which represents a filter inductor and an equivalent series resistance (ESR). Thus, the control signal is developed to emulate the reference value by tracking its dynamic response all the time. The best result is when the control signal is identical to its reference, i.e. the steady state error becomes zero. The typical PI controller usually being picked to handle the steady state error by tuning its proportional and integral gain accordingly using the conventional control approaches such as Ziegler-Nichols method, root locus, Bode plot etc. By employing Laplace tarnsform, the tuned gains of a basic PI controller transfer function both in continuous time domain and discrete time domain (z-transform) can be expressed as:

$$PI(s) = K_p + K_i/s \quad (3)$$

$$PI(z) = \frac{mz-n}{z-1} \quad (4)$$

Where K_p and K_i are the proportional gain and the integral gain of PI controller respectively. On the other hand m and n are the coefficients for the discrete PI controller. Normally, the PI(s) is designed first before being transformed into PI(z) using zero order hold (ZOH) or Tustin technique [15]. Hence, the respective m and n can be described in K_p and K_i terms as:

$$m = 2K_p + K_iT \quad (5)$$

$$n = K_iT - 2K_p \quad (6)$$

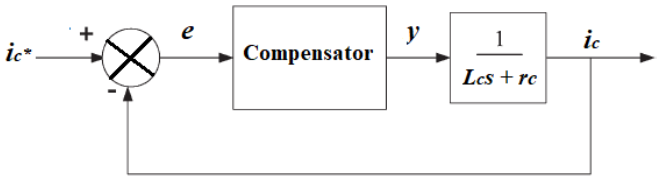

Figure 2: Closed loop control for compensated current

The mathematical expression for the PL-LTC based SIFPIC compensator using a difference equation is:

$$y(k) = n\left[\frac{m+n}{n}e(k) + \big(e(k) - e(k-1)\big)\right] + y(k-1) \quad (7)$$

A block diagram that illustrates the PL-LTC based SIFPIC design in MATLAB Simulink environment is depicted in Figure 3. Hence, the slope λ is equal to:

$$\lambda = \frac{m+n}{n} \quad (8)$$

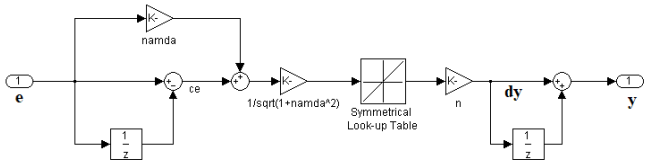

Figure 3: FPIC design in MATLAB Simulink environment

2.3 SAPF Control Strategy

Figure 4 shows the voltage source inverter SAPF connected to the AC system at a point of common coupling (PCC). It is located before the nonlinear load which is a diod rectifier with inductive load (series connection of inductor and resistor). At the PCC, the instantaneous currents flow can be written as:

$$i_L = i_c + i_s \quad (9)$$

And the source voltage is given as:

$$v_s = V_m \sin \omega t \quad (10)$$

In order to mitigate harmonic component in the source current and improve the system power factor, the DCC method shows in Figure 5 is chosen as the preferred current control method. Usually the load current which have fundamental and harmonic components is filtered according to control strategy proposed in [7] and depicted in Figure 6. Instead of applying the AC load current and source voltage, the DC load current and voltage are selected as the input of the control strategy. Hence,

$$|i_L| = i_o = i_f + i_h + i_q \quad (11)$$

Thus, the compensated current is desired to inject a harmonic and reactive component of the load current which is identical and equal in magnitude but opposite in polarity to the line at the PCC. It actively shaping the source current so that the source current is free from harmonic and reactive power component. The only thing left is the fundamental component in the source current that obviously a sine waveform, identical to the source voltage and in phase with it. Therefore, the compensated source current can be expressed as follows:

$$i_c = -i_h - i_q \quad (12)$$

$$i_s = i_o - i_c = i_o - i_h - i_q = i_f \quad (13)$$

where i_L: AC load current, i_o: DC load current, i_c: compensated current, i_h: harmonic current, and i_q: reactive power current. Table 3 lists the system parameter used in the simulation.

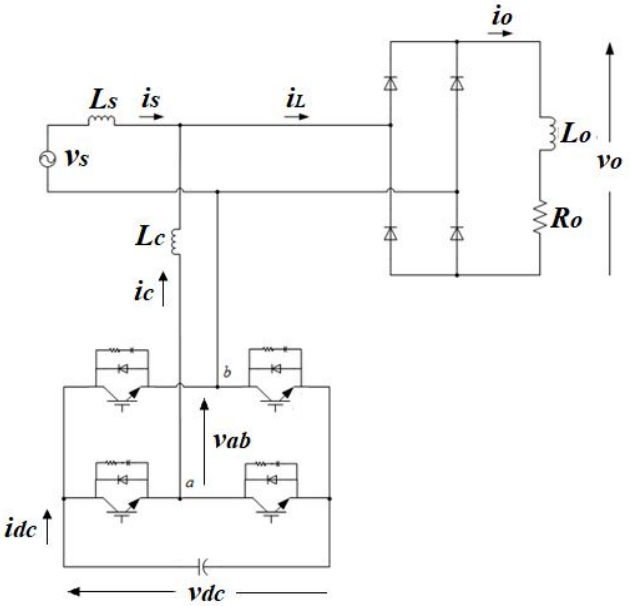

Figure 4: AC system with SAPF and nonlinear load

According to the control strategy proposed in [7], firstly the DC load current, i_o and voltage, v_o are measured separately and before both quantities simultaneously being low-pass filtered to yield their respective average DC values. To calculate the equivalent resistance, R_e the average DC voltage, V_o divided the average DC current, I_o. Later, this value is being used to produce the sinusoidal reference current, i_s^*. Lastly, the aforementioned reference is subtracted by the load current, i_L to obtain the desired compensated reference current, i_c^*. Actually, the proposed compensator is employed at the second stage, where the PWL-LTC controller gains are tuned accurately to yield the control signal, y. The final stage is the switching scheme, where a linear bipolar pulse width modulation (PWM) technique is implemented to attain the gating signals, g for power switches operation.

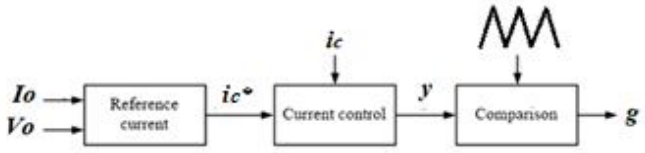

Figure 5: Direct current control method for SAPF

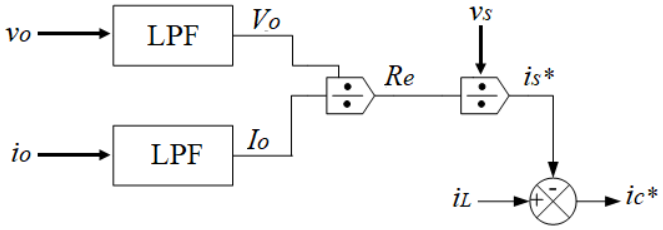

Figure 6: SAPF control strategy proposed in [7]

Table 3: System parameter

Parameter	Value
Source voltage	V_s = 110 V_{rms}
System frequency	f_1 = 50 Hz
Line impedance	L_s = 0.5 mH, R_s = 0.05 Ω
Nonlinear load	L_o = 50 mH, R_o = 20 Ω
SAPF storage elements	C_{dc} = 470 µF, L_c = 3.0 mH, r = 0.1 Ω
Switching frequency	f_s = 20 kHz
PI gains	K_p = 3.2, K_i = 1824
SIFPIC gains	λ = 1.0, m = 3.208, n = 3.199
Sampling time	T = 5 µs

3. RESULTS AND DISCUSSION

The SAPF circuit, the AC system and the nonlinear load are modelled and simulated using MATLAB Simulink tool. Many researchers implemented MATLAB Simulink to model and simulate electrical circuits [8]-[25]. In this case, the simulation runs on discrete solver for a duration of 2.5 s. There are three simulation tests carried out to validate the performance and effectiveness of the proposed controller for SAPF application. Figure 7 shows the bar plot for harmonic spectrum of source current with and without SAPF. The harmonic spectrum starts from the 1st order until 30th order, and each single harmonic indicates a uniform drop from the start until the end before the SAPF being applied. The THD without SAPF is 28.7%, thus justifies the source current waveform which owns considerable harmonic distortion. Nevertheless, after SAPF connection, the THD of source current becoming better when it recorded only 3.07%, a value

below 5.0%, a standard specification set by IEEE 519. Moreover, the fundamental harmonic has been increased from 6.8 A before filtering to 8.2 A after filtering. It is an increment of 1.4 A, which result in higher active power for the system. The rest of harmonic orders show a significant reduction in their magnitudes after filtering using SAPF. These are obvious for dominant harmonics.

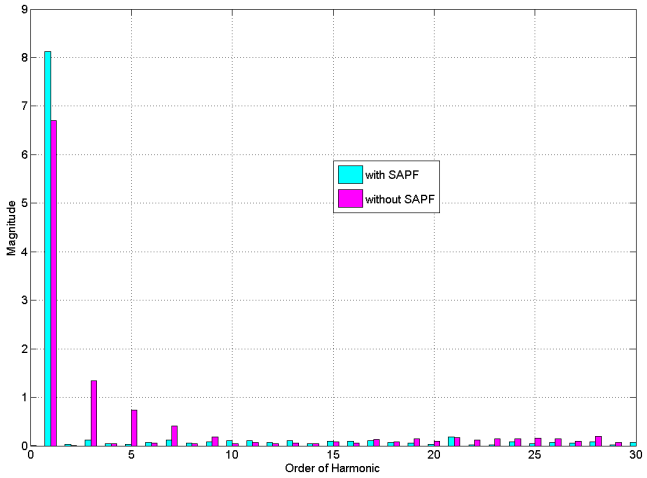

Figure 7: Source current THD spectrum up to 30th harmonic

On the other hand, Figure 8 depicts some important variables at steady state in order to investigate the performance of PL-LTC based SIFPIC for harmonic mitigation. By observation from top to bottom, there is no change happened to the source voltage after SAPF connection. The source current also looks sinusoidal wave, identical to the source voltage. Besides it is in phase with the source voltage. Its amplitude is 8.2 A, same as the magnitude measured for fundamental harmonic. Next, the load current has no sign of change, except its ripple has been increased a little. Hence, the SAPF cannot mitigate the harmonic component of load current, because the control strategy is created to solve the source current problem only. The compensated current waveform has more distortion than the rest. Actually, the THD in compensated current is the highest among those three current variables [4], since it is purely containing harmonic and reactive power components. Without any perturbation on the system, the DC-bus voltage constantly retains its value around 400 V. Meaning that the power flow between the supply and the load is balance. Notice that there is no regulation is imposed on the DC-bus voltage, hence the control requires only a single loop rather than a double loop like reported in [2]. Finally, the system active power exhibits a constant value at 600 W and the reactive power close to 0 Var. Therefore, the SAPF able to improve the system active power and compensate the reactive power.

In order to compare the performance of the proposed controller, the PI controller was also implemented. As a result, all variables indicate identical waveforms like the proposed controller but slightly less performance, especially the source current THD index and the DC-bus voltage, v_{dc} magnitude. The THD is recorded at 4.96%, slightly higher than the THD of 3.07% for PL-LTC controller. Hence, both controllers successfully meet the specified IEEE-519 standard. The v_{dc} used higher voltage means the better active power supply as well as the superior switching losses compensation of SAPF.

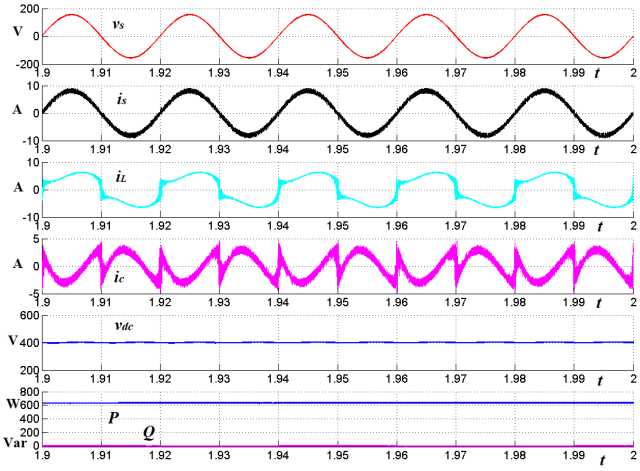

Figure 8: (From top to bottom); Source voltage, source current, load current, compensated current, DC-bus voltage, and active power with reactive power waveforms using PL-LTC controller

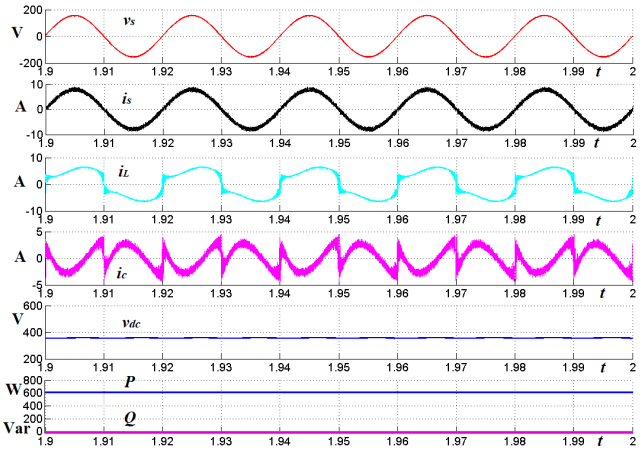

Figure 9: (From top to bottom); Source voltage, source current, load current, compensated current, DC-bus voltage, and active power with reactive power waveforms using PI controller

Figure 10 indicates similar results as Figure 8, albeit the simulation taken is longer and it includes a loading perturbation occurred at 1.2 s. This is done in order to investigate the dynamic response of the proposed controller. From top to bottom, there is no sign of change occurred on the source voltage even during the moment of loading perturbation. However, the source current needs around 5 cycles before reaching a new steady state value after the loading perturbation. It increased from amplitude of 8.2 A to 16. 4 A since the DC load resistance being lowered from 20 Ω to 10 Ω. At steady state, the source current THD after the loading step up has improved from 3.07% to 2.96%. Thus, the SAPF works better with higher resistance for inductive load.

The load current and compensated current immediately varied to a higher value during the loading perturbation. Their magnitude also climbed up to twice a value of the previous one. Compared to the source current, both have faster dynamic response rates because of the DC-bus voltage effect which it is not regulated. It is confirmed by the time lag of 0.7 s measured at the DC-bus voltage dynamic response rate before it reached a settling time past the loading step up instant. The increment of 200 V is achieved from 400 V before to 600 V after the loading step up. The reason of more DC voltage supply needed by the load is owing to the load's active power demands increased suddenly. This evidence is shown via the system active power response after the loading perturbation. It doubles up from 600 W to 1200 W in order to reflect the loading step up. The time taken to take effect is less than 0.3 s. Nevertheless, the reactive power maintains its value at near 0 Var even though the load rose up to double figures. This is due to the SAPF effective filtering notwithstanding the sudden load perturbation.

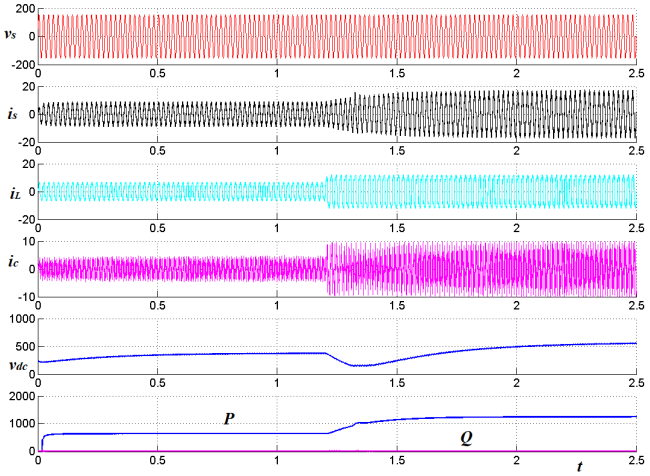

Figure 10: (From top to bottom); Source voltage, source current, load current, compensated current, DC-bus voltage, and active power with reactive power waveforms

To summarize the findings, Table 4 indicates the THD and system power factor performances with and without SAPF installation. It also compares the findings of using PL-LTC SIFPIC controller and PI controller. Apparently, the proposed controller gives better performance than the PI controller.

Table 4: Controllers performance comparison

Test	THD	Power factor
Before filtering:	28.7%	0.961
After filtering: PL-LTC SIFPIC controller – Normal condition Step up loading	 3.07% 2.96%	 0.9996 0.9995
PI controller – Normal condition	 4.96%	 0.9988

To verify further, particularly in term of parameters and features comparison between the proposed controller and the SIFPIC controller developed by Suresh and Singh [2], Table 5 is formed. Obviously, in term of performance-wise both are equaled, but the proposed controller structure is much simpler since it does not have a peak detector and the mathematical expression to derive the reference currents is more concise.

Table 5: SIFPIC controller comparison

Parameter/Feature	Proposed	Paper [2]
Current control method	DCC	ICC
DC voltage regulation	No	Yes
Current compensation	Yes	No
Switching scheme	PWM	Hysteresis
System phase	Single	Three
Peak detector	No	Yes
Low-pass filter	Yes	No
Sensor count	Three	Three
Experimental results	No	Yes

4. CONCLUSION

This paper inclusively discussing about the design, application and performance of a compensator based on PL-LTC SIFPIC for the SAPF control strategy proposed in [7]. The proposed compensator shows its potential and promising feature as the alternative compensator for the power quality improvement of a single-phase system with nonlinear loads. All the objectives have been met and it successfully mitigates the harmonic content of source current significantly from 28.7% to 3.07% and 2.96% respectively. Thus, both controllers meet the IEEE 519 standard. Besides, the power factor of the system also improved to near unity as indicated in Table 4.

Indeed, a good control strategy for the SAPF is required in resolving the issues related to current or voltage harmonic distortion. Presently, there are many types of compensator available and having been used by the SAPF but most of them is based on PI controller. A new compensator, namely PL-LTC SIFPIC which enhanced and upgraded the capability of PI controller is introduced using nonlinear load equivalent resistance estimation control strategy for SAPF application. Simulation results validate the performance and effectiveness of the proposed compensator. The findings can be improved further if the tuning of PI controller gains is more precise and accurate. Moreover, the approximation using piecewise linear look-up table can also be enhanced if a nonlinear piecewise look-up table is employed. In addition to the simulation-based verification, an actual evidence of the proposed controller effectiveness via experimental investigation could be implemented in the future.

ACKNOWLEDGEMENT

The authors would like to express gratitude and thankful towards the Universiti Kebangsaan Malaysia because providing a research grant, GGPM-2019-061.

REFERENCES

1. S. K. Jain, P. Agrawal, and H. O. Gupta. **Fuzzy logic controlled shunt active power filter for power quality improvement**. *IEE Proc. Electr. Power Appl*., vol. 149, no. 5, pp. 317-328, Sep. 2002. https://doi.org/10.1049/ip-epa:20020511
2. D. Suresh, and S. P. Singh. **Design of single input fuzzy logic controller for shunt active power filter**, *IETE Journal of Research*, vol. 61, no.5, pp. 500-509, 2015. https://doi.org/10.1080/03772063.2015.1024176
3. H. Akagi. **Active harmonic filters**. *Proc. of the IEEE*, vol. 93, no. 12, pp. 2128-2141, 2005. https://doi.org/10.1109/JPROC.2005.859603
4. Y. Yusof, R. Zaim, and N. A. Rahim. **Single-phase active power filter using a simple control strategy**. *Jurnal Teknologi (Sciences & Engineering)*, vol. 79, no. 6, pp. 45-52, 2017.
5. L. Asiminoaei, F. Blaabjerg, and S. Hansen. **Detection is key – Harmonic detection methods for active power filter applications**. *IEEE Industry Applications Magazine*, vol. 13, no. 4, pp. 22-33, 2007. https://doi.org/10.1109/MIA.2007.4283506
6. M. Adel, S. Zaid, and O. Mahgoub. **Improved active power filter performance based on an indirect current control technique**. *Journal of Power Electronics*, vol. 11, no. 6, pp. 931-937, 2011. https://doi.org/10.6113/JPE.2011.11.6.931
7. Y. Yusof, R. Za'im, A. Ayob, A. M. Muad, and R. Mohamed. **Harmonic current detection method using nonlinear load's dc output voltage and current**. *2019 7th International Conference on Smart Computing and Communications, ICSCC 2019*. https://doi.org/10.1109/ICSCC.2019.8843641
8. M. A. A. M. Zainuri, M. A. M. Radzi, A. C. Soh, N. Mariun, and N. A. Rahim. **DC-link capacitor voltage control for single-phase shunt active power filter with step size error cancellation in self-charging algorithm.** *IET Power Electron*., vol. 9, Iss. 2, pp. 323–335, 2016. https://doi.org/10.1049/iet-pel.2015.0188
9. C. N. Bhende, S. Mishra, and S. K. Jain. **TS-Fuzzy-controlled active power filter for load compensation**. *IEEE Trans. Pow. Del*, vol. 21, no. 3, pp. 1459-1465, 2006. https://doi.org/10.1109/TPWRD.2005.860263
10. M. A. M. Radzi, and N. A. Rahim. **Neural network and band-less hysteresis approach to control switched capacitor active power filter for reduction of harmonics**, *IEEE Trans. Ind. Electron*., vol. 54, no. 5, pp. 1477–1484, 2009. https://doi.org/10.1109/TIE.2009.2013750
11. S. M. Ayob, N. A. Azli, and Z. Salam. **PWM dc-ac converter regulation using a multi-loop single input Fuzzy-PI controller.** *Journal of Power Electronics*, vol. 9, no. 1, pp. 124-131, 2009.
12. S. M. Ayob, Z. Salam, and N. A. Azli. **A new optimum design for a single input Fuzzy controller applied to dc to ac converters.** *Journal of Power Electronics*, vol. 10, no. 3, pp. 306-312, 2010. https://doi.org/10.6113/JPE.2010.10.3.306
13. B. J. Choi, S.W. Kwak, and B. K. Kim. **Design and stability analysis of single-input fuzzy logic controller**. *IEEE Trans. Syst., Man, Cybern.*, vol. 30, no. 2, pp. 303-309, 2000.
14. T-S. Tsay. **Adaptive piecewise linear controller for servo mechanical control systems.** *Journal of Applied Mathematics and Physics*, vol. 1, pp. 85-92, 2013. https://doi.org/10.4236/jamp.2013.15013
15. S. M. Ayob, Z. Salam, and N. A. Azli. **Simple PI Fuzzy logic controller applied in DC-AC converter**. *First International Power and Energy Conference PECon 2006, Putrajaya, Malaysia*, pp. 393-398, 2006.
16. S. Rahmani, N. Mendalek, and K. Al-Haddad. **Experimental design of a nonlinear control technique for three-phase shunt active power filter**. *IEEE Trans. Ind. Electr*., vol. 57, no. 10, pp. 3364-3375, 2010.
17. V. K. Chaithanya, A. Pandian, RBR Prakash, and C. R. Reddy. **Analysis of closed loop control of cascaded three phase grid tied inverter using Fuzzy Logic Controller**. *International Journal of Advanced Trends in Computer Science and Engineering*, vol. 8, no.4, pp. 1123 – 1127, 2019. https://doi.org/10.30534/ijatcse/2019/1984
18. N. S. Razali, N. Roslan, M. H. Mansor, I. Musirin, S. A. Shaaya, and S. Jelani. **Optimal reactive power control using compensating capacitor based on artificial immune system**. *International Journal of Advanced Trends in Computer Science and Engineering*, vol. 8, no.1, pp. 381-386, 2019. https://doi.org/10.30534/ijatcse/2019/6781.32019
19. M. R. Gopal, and S. Yarnagula. **Simulation and analysis of shunt active power filter for power quality improvement**. *International Journal of Advanced Trends in Computer Science and Engineering*, vol. 3, no.1, pp. 26 – 31, 2014.
20. R. Lakavath, M. Kishore. **Simulation and harmonic analysis of domestic loads and harmonic reduction techniques in industrial distribution system**. *International Journal of Advanced Trends in Computer Science and Engineering*, vol. 3, no.1, pp. 504-509, 2014.
21. Y. Yusof, and N. A. Rahim. **Comparative study between SPWM and THIPWM control techniques for PWM-VSI using mathematical modeling and simulation**. *J. Kejuruteraan*, vol. 23, pp. 17-26, 2011.
22. S. Rahmani, K. Al-Haddad, H. Kanaan, and F. Fnaiech. **Modified PWM with a new indirect current control technique applied to a single-phase shunt active power filter**. *Can. J. Elect. Comput. Eng*., vol. 31, no. 3, pp. 135-144, 2006. https://doi.org/10.1109/CJECE.2006.259208
23. Y. Yusof, and K. Mat. **Modeling, simulation and analysis of induction motor for electric vehicle**

application. *International Journal of Engineering and Technology (UAE)*, vol. 7, no. 3, pp. 145-150, 2018.

24. C. Chang, Y. Yuan, T. Jiang, and Z. Zhou. **Field programmable gate array implementation of a single-input fuzzy proportional–integral–derivative controller for DC–DC buck converters**. *IET Power Electronics*, vol. 9, no. 6, pp. 1259–1266, 2016.
25. T. Kumbasar. **Robust stability analysis and systematic design of single-input interval type-2 fuzzy logic controllers**. *IEEE Trans. Fuzzy Syst.*, vol. 24, no. 3, pp. 675-694, 2016. https://doi.org/10.1109/TFUZZ.2015.2471805